International Journal of Ocean System Engineering 3(1) (2013) 22-32
http://dx.doi.org/10.5574/IJOSE.2013.3.1.022

Heuristic Physical Theory of Diffraction for Impedance Polygon

Keunhwa Lee[1], Sanghyun Park[2], Kookhyun Kim[3], and Woojae Seong[1*]

[1]*Dept. of Naval Architecture and Ocean Engineering, Seoul National University, San 56-1, Sillim-dong, Kwanak-gu, Seoul 151-744, Korea*

[2]*Air wing 6, Republic of Korea Navy*

[3]*Dept. of Naval Architecture, Tongmyong University, 179, Sinseonno, Nam-gu, Busan, 608-711, Korea*

(Manuscript Received December 9 2012; Revised January 18, 2013; Accepted February 21, 2013)

Abstract

A heuristic physical theory of diffraction (PTD) for an acoustic impedance wedge is proposed. This method is based on Ufimtsev's three-dimensional PTD, which is derived for an acoustic soft or hard wedge. We modify the original PTD according to the process of physical optics (or the Kirchhoff approximation) to obtain a 3D heuristic diffraction model for an impedance wedge. In principle, our result is equivalent to Luebbers' model presented in electromagnetism. Moreover, our approach provides a useful insight into the theoretical basis of the existing heuristic diffraction methods. The derived heuristic PTD is applied to an arbitrary impedance polygon, and a simple PTD formula is derived as a supplement to the physical optics formula.

Keywords: Physical Theory of Diffraction, Kirchhoff Approximation, Impedance Polygon, Heuristic Approach, Physical Optics

1. Introduction

Diffraction may be as important as reflection in investigations of wave propagation in a complex environment or high frequency scattering from an object. Diffraction contributes to wave propagation within the shadow zone that is unreachable by reflected rays, and plays a main role in wave scattering in a non-specular direction.

Traditional high-frequency diffraction methods are usually categorized into Keller's geometrical theory of diffraction (GTD) [1], which was later modified into the uniform theory of diffraction (UTD) [2] by removing the singularity, and Ufimtsev's physical theory of diffraction (PTD) [3]. The above methods were essentially developed for the perfectly conducting wedge (the soft wedge in acoustics), which is capable of being modeled by the closed analytic solution from the *canonical wedge problem*. Subsequently, some authors have applied rigorous diffraction theory to the impedance wedge. However, most of these theories have been based on Maliuzhinets' solution [4, 5], which is expressed by a computationally intensive mathematical function and thus is not widely used in practical modeling. To address this difficulty, Luebbers [6, 7] suggested a heuristic modification to the original UTD for a non-perfectly conducting wedge, and a series of related studies on this heuristic UTD have been presented by a few authors [8-17] in the radio wave community. Although there have been no attempts to account for the physical basis of Luebbers' modification, his heuristic UTD has been practically applied in many different fields, including communication channel modeling and radar modeling. Otherwise, to our knowledge, there have been no

*Corresponding author. Tel.: ++82-2-880-7332, Fax.: ++82-2-888-9298, E-mail address: wseong@snu.ac.kr

studies on heuristic diffraction theory based on the PTD.

The objective of this paper is to develop a new heuristic PTD for the acoustic impedance wedge, along with a formula for the diffraction field of the impedance polygon. The derivation of this work differs from other UTD studies in that it follows the approach of Ufimstev's 3D PTD [3]. The derived heuristic PTD will supplement physical optics (PO) models [18-20] for an impedance object and will help clarify the validity of existing heuristic approaches. In Section 2, the heuristic PTD for an edge is formulated from the Kirchhoff-Helmholtz integral equation and compared with Luebbers' heuristic UTD. The derived heuristic PTD is then extended for the impedance polygon in Section 3. Numerical examples comparing the heuristic PTD and the rigorous solution obtained by the boundary element method are provided in Section 4. Section 5 presents the conclusions.

2. Heuristic PTD for Acoustic Impedance Wedge

2.1 PTD for Soft or Hard Wedge

The physical theory of diffraction (PTD) [3, 12] is a high-frequency asymptotic technique applied to wave diffraction/scattering. The PTD considers a scattering field that consists of radiation from elementary sources distributed on an object's surface. These elementary sources are divided into both uniform and non-uniform sources. The uniform sources are induced on the object's surface by the Kirchhoff approximation (KA). All of the other sources are considered to be non-uniform sources, and they are concentrated near the edges.

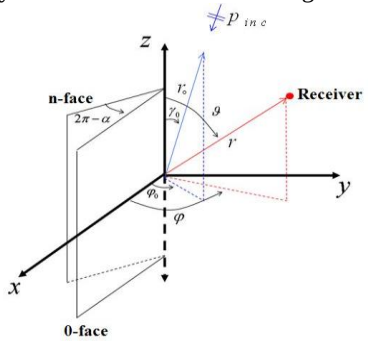

Fig. 1. Basic coordinate system used for wedge.

Consider an oblique incident plane wave p^{inc} in relation to a soft or hard wedge (Fig. 1). The 0-face of the wedge is parallel to the xz-plane in a rectangular coordinate system, and the n-face is folded as the wedge's external angle α, greater than π. p^{inc} is incident on the edge with bearing angle φ_0 and elevation angle γ_0. The receiver is oriented with bearing angle φ and elevation angle ϑ. The incident wave is defined as $p_0 e^{-jkz\cos\gamma_0} e^{-jk_1 r\cos(\varphi-\varphi_0)}$, where k is the medium wave number and $k_1 = k\sin\gamma_0$; then, the total wave field $p^t_{s,h}$ is respectively expressed for a soft or hard wedge as follows [3].

$$p^t_{s,h}(r,\varphi) = p_0 e^{jkz\cos\gamma_0}[v(k_1 r,\varphi-\varphi_0) \mp v(k_1 r,\varphi+\varphi_0)] + p^{go}_{s,h}(r,\varphi) \tag{1}$$

where $v(k_1 r,\psi) = \frac{1}{2\alpha}\int_D \frac{e^{-jk_1 r\cos\eta}}{1-e^{j[\pi(\eta+\psi)/\alpha]}}d\eta$ using Sommerfeld's integral contour D [22], and $p^{go}_{s,h}$ represents the geometrical plane waves composed of the incident and reflected plane waves.

The uniform sources $j^{(0)}_{s,h}$ for a soft or hard wedge are expressed by KA as follows.

$$j^{(0)}_s = \frac{\partial p^{inc}}{\partial n} + \frac{\partial p^{ref}_s}{\partial n} = 2\frac{\partial p^{inc}}{\partial n},$$
$$j^{(0)}_h = p^{inc} + p^{ref}_h = 2p^{inc} \text{ on the illuminated surface} \tag{2}$$

where $\partial/\partial n$ is the normal derivative for the surface.

The non-uniform sources are defined using Eq. (1) as follows.

$$j^{(1)}_s = \frac{\partial p^t_s}{\partial n} - j^{(0)}_s$$
$$= \partial\left(p_0 e^{jkz\cos\gamma_0}[v(k_1 r,\varphi-\varphi_0) \mp v(k_1 r,\varphi+\varphi_0)]\right)/\partial n$$
$$\text{at } \varphi = 0,\alpha \tag{3}$$

and

$$\begin{aligned} j_h^{(1)} &= p_h^t - j_h^{(0)} \\ &= p_0 e^{jkz\cos\gamma_0}[v(k_1 r, \varphi-\varphi_0) \mp v(k_1 r, \varphi+\varphi_0)] \\ &\text{at } \varphi=0,\alpha \end{aligned} \tag{4}$$

Then, the physical optics (PO) and PTD field are calculated using the radiation integral for the object surface as follows.

$$\begin{aligned} p_s^{(0)} &= -\frac{1}{4\pi}\int_{S_B'} j_s^{(0)} \frac{e^{jk|r'-r|}}{|r'-r|} dS_B', \\ p_h^{(0)} &= \frac{1}{4\pi}\int_{S_B'} j_h^{(0)} \frac{\partial}{\partial n}\left(\frac{e^{jk|r'-r|}}{|r'-r|}\right) dS_B' \end{aligned} \tag{5}$$

And

$$\begin{aligned} p_s^{(1)} &= -\frac{1}{4\pi}\int_{S_B'} j_s^{(1)} \frac{e^{jk|r'-r|}}{|r'-r|} dS_B', \\ p_h^{(1)} &= \frac{1}{4\pi}\int_{S_B'} j_h^{(1)} \frac{\partial}{\partial n}\left(\frac{e^{jk|r'-r|}}{|r'-r|}\right) dS_B' \end{aligned} \tag{6}$$

where $|r'-r|$ is the distance between the receiver position vector r and the position vector on the object surface S_B', r'.

The non-uniform source in Eq. (6) includes a complex integral and is difficult to calculate. To simplify Eq. (6), Ufimtsev adopts the integral approximation of the stationary phase method together with an analytic calculation of the complex integral, which produces a line integral for the differential edge between two faces. Then, Eq. (6) is written as

$$\begin{aligned} p_s^{(1)} &= \frac{1}{2\pi}\int_L p^{inc}(\varsigma) F_s^{(1)}(\vartheta,\varphi)\frac{e^{jkR}}{R} d\varsigma \\ p_h^{(1)} &= \frac{1}{2\pi}\int_L p^{inc}(\varsigma) F_h^{(1)}(\vartheta,\varphi)\frac{e^{jkR}}{R} d\varsigma \end{aligned} \tag{7}$$

where L is the edge of the wedge, ς is the curvilinear coordinate along the edge, and R is the distance between the position vector of the receiver and the position vector of the differential edge. The PTD diffraction coefficients $F_s^{(1)}(\vartheta,\varphi)$ and $F_h^{(1)}(\vartheta,\varphi)$ and their related parameters are given in Appendix A.

Eq. (7) appears to be limited to the canonical acoustic wedge, which is paradoxical since the wedge has an infinite edge length. We address this by adopting the asymptotic localization principle for the high frequency range, such that the non-uniform sources are asymptotically equivalent to the components induced on the canonical wedge tangent to the real edge. Then, Eq. (7) is applicable to arbitrary smooth edges of finite length.

2.2 Heuristic PTD for Impedance Wedge

Consider the Kirchhoff-Helmholtz integral equation for the external scattering from an object [23].

$$\begin{aligned} p^s = \frac{1}{4\pi}\int_{S_B'} [\, & p^t(r'|r_0)\frac{\partial}{\partial n}\left(\frac{e^{jk|r-r'|}}{|r-r'|}\right) \\ & - \frac{e^{jk|r-r'|}}{|r-r'|}\frac{\partial p^t(r'|r_0)}{\partial n}] dS_B' \end{aligned} \tag{8}$$

where r_0 is the source position vector, and $p^t = p^s + p^{inc}$ is the total wave field for an impedance object with scattering wave field p^s and incident wave field p^{inc}.

By the Kirchhoff approximation for the impedance wedge, the PO field is obtained with the plane wave reflection coefficient $\hat{R}$, and is given by

$$\begin{aligned} p^{s(0)} = \frac{1}{4\pi}\int_{S_B'} [\, & (1+\hat{R}) p^{inc}(r'|r_0)\frac{\partial}{\partial n}\left(\frac{e^{jk|r-r'|}}{|r-r'|}\right) \\ & - (1-\hat{R})\frac{e^{jk|r-r'|}}{|r-r'|}\frac{\partial p^{inc}(r'|r_0)}{\partial n}] dS_B' \end{aligned} \tag{9}$$

where S_B' represents the illuminated wedge surface. Notice that the reflection coefficient is a function of the grazing angle, which is the acute angle between the incident wave direction vector and its

orthogonally projected vector on the object surface. When both faces of the wedge are illuminated, two reflection coefficients for the 0-face and n-face have to be used.

Comparing the above equation with Eq. (5) for a soft or hard wedge, we observe that the PO field for an impedance object is created by two types of uniform sources. The first is a monopole-type source equivalent for a soft wedge, and the other is a dipole-type source for a hard wedge. Let each uniform source be defined as

$$j_m^{(0)} = (1-\hat{R})\frac{\partial p^{inc}(r'\,|\,r_0)}{\partial n},\ j_d^{(0)} = (1+\hat{R})\,p^{inc}(r'\,|\,r_0) \text{ on the illuminated part} \tag{10}$$

The equivalent total wave fields for the impedance wedge, corresponding to the monopole-type and dipole-type uniform sources of Eq. (10), may be respectively designed with the plane reflection coefficient defined in the PO field, so that

$$p_m^t(r,\varphi) = \left(\frac{1-\hat{R}}{2}\right) p_0 e^{jkz\cos\gamma_0}[v(k_1 r,\varphi-\varphi_0)\mp v(k_1 r,\varphi+\varphi_0)] + j_m^{(0)} \tag{11}$$

and

$$p_d^t(r,\varphi) = \left(\frac{1+\hat{R}}{2}\right) p_0 e^{jkz\cos\gamma_0}[v(k_1 r,\varphi-\varphi_0)\mp v(k_1 r,\varphi+\varphi_0)] + j_d^{(0)} \tag{12}$$

The geometric field in Eqs. (11) and (12) is assumed to be equal to that obtained by the Kirchhoff approximation, and the diffraction field is converted into the diffraction field for a soft or hard wedge when $\hat{R} = -1 \text{ or } 1$. This is the only rule used to design our heuristic PTD. Furthermore, it should be noted that there can be many heuristic models based on how the rigorous field for an impedance wedge is described. For example, in the above equations, $\hat{R}$ need not be the physical reflection coefficient. Any function with greater accuracy can be applied to Eqs. (11) and (12) instead.

The non-uniform sources can be written as follows.

$$j_m^{(1)} = \frac{\partial(p_m^t - j_m^{(0)})}{\partial n},\quad j_d^{(1)} = p_d^t - j_d^{(0)} \text{ at } \varphi=0,\alpha \tag{13}$$

When these non-uniform sources are inserted into the radiation integral equation, the result is

$$p^{s(1)} = \frac{1}{4\pi}\int_{S_B'}[\,j_d^{(1)}\frac{\partial}{\partial n}\left(\frac{e^{jk|r-r'|}}{|r-r'|}\right) - j_m^{(1)}\frac{e^{jk|r-r'|}}{|r-r'|}]dS_B' \tag{14}$$

where S_B' is the total surface of the wedge.

Eq. (14) can be further simplified using the PTD described in Section 2.1. The final equation for the PTD field is expressed as

$$p^{s(1)} = \frac{1}{2\pi}\int_L p^{inc}(\varsigma)F_{im}^{(1)}(\vartheta,\varphi)\frac{e^{jkR}}{R}d\varsigma \tag{15}$$

Here, $F_{im}^{(1)} = F_d^{(1)} + F_m^{(1)}$ and the heuristic coefficients $F_d^{(1)}$ and $F_m^{(1)}$ are obtained as follows.

$$F_d^{(1)}(\vartheta,\varphi) = -\frac{1}{2}[(1+\hat{R}_0)V(\sigma_1,\varphi_0)\sin\varphi + (1+\hat{R}_n)V(\sigma_2,\alpha-\varphi_0)\sin(\alpha-\varphi)]\sin\gamma_0\sin\vartheta \tag{16}$$

and

$$F_m^{(1)}(\vartheta,\varphi) = -\frac{1}{2}[(1-\hat{R}_0)U(\sigma_1,\varphi_0) + (1-\hat{R}_n)U(\sigma_2,\alpha-\varphi_0)]\sin^2\gamma_0 \tag{17}$$

where the reflection coefficient $\hat{R}_0$ is for the 0-face and $\hat{R}_n$ is for the n-face.

Finally, the total wave field for an impedance wedge can be obtained as the sum of the PO field of Eq. (9) and the PTD field of Eq. (15).

2.3 Comparison with Luebbers' UTD model

Luebbers' model is based on the two-dimensional

UTD model for a perfectly conducting wedge. This model overcomes the singularity problem of GTD on the reflection/shadow boundary by introducing the Fresnel integral. The heuristic diffraction coefficient of Luebbers' model is shown in Appendix B. In this section, the physical origin of Luebbers' model is examined by comparing it with our heuristic PTD coefficients.

We start by transforming the 3D coefficients of Eqs. (16) and (17) into 2D coefficients. Consider that $0 \le \varphi \le \pi$ and the scattering direction lies on the Keller cone ($\vartheta = \pi - \gamma_0$). Then, the heuristic 3D PTD coefficients $F_{m,d}^{(1)}$ are transformed by Eqs. (A.1)–(A.8) into

$$\begin{aligned} F_m^{(1)}(\frac{\pi}{2}-\gamma_0,\varphi) = & -\frac{\pi(1-\hat{R}_0)}{4\alpha}\left[\cot\left(\frac{\pi-(\varphi-\varphi_0)}{2\alpha/\pi}\right)-\cot\left(\frac{\pi-(\varphi+\varphi_0)}{2\alpha/\pi}\right)\right] \\ & -\frac{\pi(1-\hat{R}_n)}{4\alpha}\left[\cot\left(\frac{\pi+(\varphi-\varphi_0)}{2\alpha/\pi}\right)-\cot\left(\frac{\pi+(\varphi+\varphi_0)}{2\alpha/\pi}\right)\right] \\ & -\frac{\varepsilon(\varphi_0)(1-\hat{R}_0)}{4}\left[\cot\left(\frac{\pi-(\varphi-\varphi_0)}{2}\right)-\cot\left(\frac{\pi-(\varphi+\varphi_0)}{2}\right)\right] \\ & -\frac{\varepsilon(\alpha-\varphi_0)(1-\hat{R}_n)}{4}\left[\cot\left(\frac{\pi+(\varphi-\varphi_0)}{2}\right)-\cot\left(\frac{\pi+(\varphi+\varphi_0)}{2}\right)\right] \end{aligned} \tag{18}$$

and

$$\begin{aligned} F_d^{(1)}(\frac{\pi}{2}-\gamma_0,\varphi) = & -\frac{\pi(1+\hat{R}_0)}{4\alpha}\left[\cot\left(\frac{\pi-(\varphi-\varphi_0)}{2\alpha/\pi}\right)+\cot\left(\frac{\pi-(\varphi+\varphi_0)}{2\alpha/\pi}\right)\right] \\ & -\frac{\pi(1+\hat{R}_n)}{4\alpha}\left[\cot\left(\frac{\pi+(\varphi-\varphi_0)}{2\alpha/\pi}\right)+\cot\left(\frac{\pi+(\varphi+\varphi_0)}{2\alpha/\pi}\right)\right] \\ & -\frac{\varepsilon(\varphi_0)(1+\hat{R}_0)}{4}\left[\cot\left(\frac{\pi-(\varphi-\varphi_0)}{2}\right)+\cot\left(\frac{\pi-(\varphi+\varphi_0)}{2}\right)\right] \\ & -\frac{\varepsilon(\alpha-\varphi_0)(1+\hat{R}_n)}{4}\left[\cot\left(\frac{\pi+(\varphi-\varphi_0)}{2}\right)+\cot\left(\frac{\pi+(\varphi+\varphi_0)}{2}\right)\right] \end{aligned} \tag{19}$$

In the above equations, the first and second terms result from the canonical wedge solution, while the third and fourth terms are contributed from the physical optics term.

The 2D heuristic PTD coefficient $F_{im}^{(1)}(\pi/2-\gamma_0,\varphi)$ is calculated as the sum of $F_m^{(1)}$ and $F_d^{(1)}$ as follows.

$$\begin{aligned} F_{im}^{(1)}(\frac{\pi}{2}-\gamma_0,\varphi) = & -\frac{\pi}{2\alpha}\left[\cot\left(\frac{\pi-(\varphi-\varphi_0)}{2\alpha/\pi}\right)+\hat{R}_0\cot\left(\frac{\pi-(\varphi+\varphi_0)}{2\alpha/\pi}\right)\right] \\ & -\frac{\pi}{2\alpha}\left[\cot\left(\frac{\pi+(\varphi-\varphi_0)}{2\alpha/\pi}\right)+\hat{R}_n\cot\left(\frac{\pi+(\varphi+\varphi_0)}{2\alpha/\pi}\right)\right] \\ & -\frac{\varepsilon(\varphi_0)}{2}\left[\cot\left(\frac{\pi-(\varphi-\varphi_0)}{2}\right)+\hat{R}_0\cot\left(\frac{\pi-(\varphi+\varphi_0)}{2}\right)\right] \\ & -\frac{\varepsilon(\alpha-\varphi_0)}{2}\left[\cot\left(\frac{\pi+(\varphi-\varphi_0)}{2}\right)+\hat{R}_n\cot\left(\frac{\pi+(\varphi+\varphi_0)}{2}\right)\right] \end{aligned} \tag{20}$$

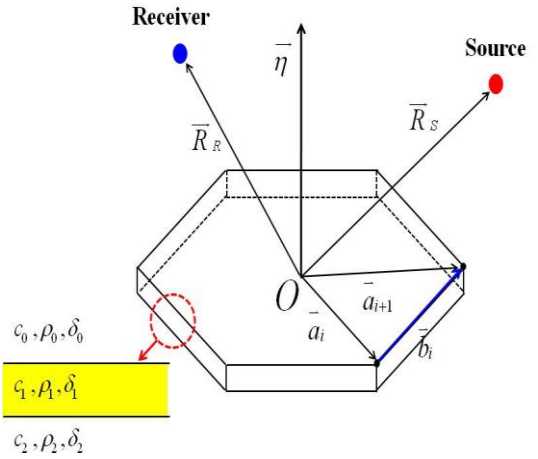

Fig. 2. Definition of coordinate system and vectors used for general definition of coordinate system.

Comparing the above equation to Luebbers' Eq. (B.1), it can be observed that they have similar structures, with the exception of the physical optics terms in our PTD model and the Fresnel integral in Luebbers' UTD model (which was used to remove the diffraction coefficient singularity). This allows us to conclude that Luebbers' model is essentially similar to the 2D reduction form of our PTD model, and is also based on the equivalent impedance wedge solution expressed by Eqs. (11) and (12).

One difference between them is the definition of the grazing angle in the 0-face and the n-face reflection coefficients. Our model's reflection coefficients are a function of the real grazing angle between the incident wave vector and its orthogonally projected vector on the 0-face or n-face, while Luebbers considers $\hat{R}_0$ to be a function of φ_0 and $\hat{R}_n$ to be a function of $\alpha - \varphi$.

As described in Section 2.2, since the reflection coefficient in the heuristic diffraction coefficient can be modified to improve the prediction, it is difficult to determine which is correct. To examine its validity, a numerical example is provided in Section 4. .

3. PTD Formula for Acoustic Impedance Polygon

In this section, the heuristic PTD is applied to the impedance polygon, and a simple formula for the PTD field is derived. This PTD formula is used to address the PO's shortcomings.

As in [24], consider a polygon facet with n vertices, as shown in Fig. 2. The edges of this polygon are connected to the edges of neighboring polygons (not shown in the figure). We define $\vec{R}_R$ to be the vector drawn from the origin of the facet to the receiver point, $\vec{R}_S$ to be the vector drawn from the origin of the facet to the source point, and $\vec{a}_i$ to be the vector drawn from the origin of the facet to the i th vertex. Also, $\vec{b}_i = \vec{a}_{i+1} - \vec{a}_i$ with $\vec{a}_{n+1} = \vec{a}_1$.

The line vector equation for the i th edge is $\vec{\varsigma}_i = (\vec{a}_i + \vec{a}_{i+1})/2 + \vec{b}_i t$ ($-0.5 \le t \le 0.5$). Then, the vector from the point of the i th edge to the receiver point is $\vec{R}_{Rd_i} = \vec{R}_R - \vec{\varsigma}_i$, and the vector from the point of the i th edge to the source point is $\vec{R}_{Sd_i} = \vec{R}_S - \vec{\varsigma}_i$.

Consider from the spherical wave field that $p^{inc} = e^{jk|\vec{R}_{Sd_i}|}/(4\pi|\vec{R}_{Sd_i}|)$ is incident on the i th edge. The PTD field in the receiver point is obtained using Eq. (15) by

$$p_i^{s(1)} = \int_{|\vec{b}_i|} \frac{e^{jk|\vec{R}_{Sd_i}|}}{4\pi|\vec{R}_{Sd_i}|} 2F_{im}^{(1)}(\vartheta_i, \varphi_i) \frac{e^{jk|\vec{R}_{Rd_i}|}}{4\pi|\vec{R}_{Rd_i}|} d\varsigma_i \qquad (21)$$

We define

$\vec{R}_{Sc_i} = \vec{R}_S - (\vec{a}_i + \vec{a}_{i+1})/2$, $\vec{R}_{Rc_i} = \vec{R}_R - (\vec{a}_i + \vec{a}_{i+1})/2$, $\vec{\zeta}_i = -\vec{R}_{Sc_i}/|\vec{R}_{Sc_i}|$, $\vec{R}_{n_i} = \vec{R}_{Rc_i}/|\vec{R}_{Rc_i}|$, and $\vec{w}_i = \vec{\zeta}_i - \vec{R}_{n_i}$. Then using the far field assumption, Eq. (21) is calculated by

$$\begin{aligned} p_i^{s(1)} &\approx \frac{2F_{im}^{(1)}(\vartheta_i, \varphi_i) e^{jk(R_{Sd_i} + R_{Rd_i})}}{(4\pi)^2 R_{Sd_i} R_{Rd_i}} \int_{|\vec{b}_i|} e^{jk(\vec{w}_i \cdot \vec{b}_i)t} d\varsigma_i \\ &= \frac{2F_{im}^{(1)}(\vartheta_i, \varphi_i) e^{jk(R_{Sd_i} + R_{Rd_i})}}{(4\pi)^2 R_{Sd_i} R_{Rd_i}} \int_{-0.5}^{0.5} |\vec{b}_i| e^{jk(\vec{w}_i \cdot \vec{b}_i)t} dt \\ &= \frac{2F_{im}^{(1)}(\vartheta_i, \varphi_i) e^{jk(R_{Sd_i} + R_{Rd_i})}}{(4\pi)^2 R_{Sd_i} R_{Rd_i}} |\vec{b}_i| \operatorname{sinc}\left(\frac{k(\vec{w}_i \cdot \vec{b}_i)}{2}\right) \end{aligned} \qquad (22)$$

where X represents $|\vec{X}|$.

With the PTD field for the i th edge, the total PTD field for a polygon facet with n edges is writ-

ten as follows:

$$p^{s(1)} = \frac{1}{(4\pi)^2} \sum_{i=1}^{n} 2|\vec{b_i}| F_{im}^{(1)}(\vartheta_i, \varphi_i) \mathrm{sinc}\left(\frac{k(\vec{w_i}\cdot\vec{b_i})}{2}\right) \frac{e^{jk(R_{Sd_i}+R_{Rd_i})}}{R_{Sd_i} R_{Rd_i}} \quad (23)$$

The above equation is the formula for the PTD field corresponding to the PO field for an impedance polygon as described in [3].

4. Numerical Results

In this section, we demonstrate the usefulness of the proposed heuristic PTD formulation by comparing the results of the three solutions for the 2D acoustic impedance wedge, using Luebbers' diffraction coefficient, our newly proposed version, and the rigorous diffraction coefficient (i.e., Maliuzhinets' solution) as a reference.

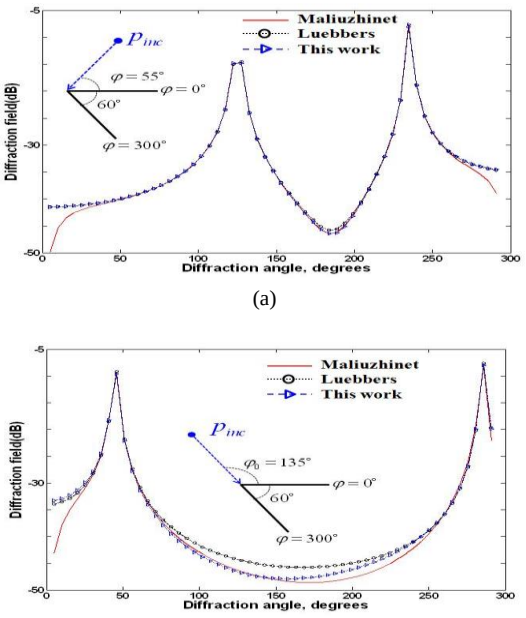

Fig. 3. Comparison of different diffraction fields for wedge angle α = 300°.
(a) Incident angle φ_0 = 55° (one face) and (b) Incident angle φ_0 = 135° (two faces).

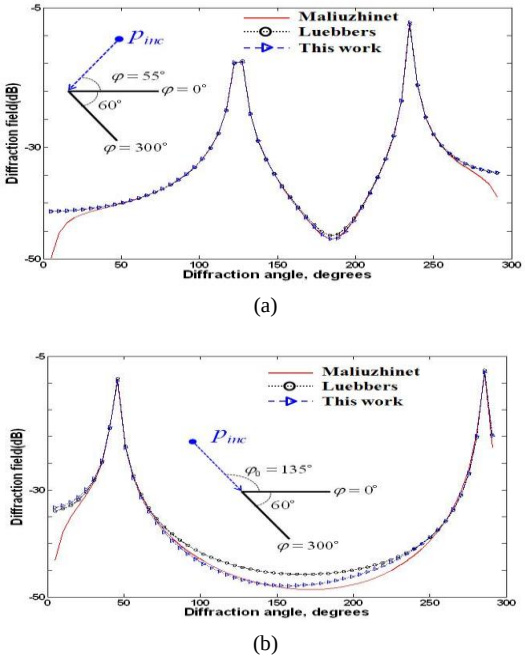

Fig. 3. Comparison of different diffraction fields for wedge angle α = 300°.
(a) Incident angle φ_0 = 55° (one face) and (b) Incident angle φ_0 = 135° (two faces).

We consider the source illumination on one or two faces of the wedge. The wedge is characterized by ρ = 2300 m^3/kg and c = 5600 m/s (glass). The medium outside the wedge is characterized by ρ = 1000 m^3/kg and c = 1500 m/s (water). A 5-kHz frequency source is located 100 m from the edge of the wedge, and the observation points are located around an arc in steps of 5° with a radius of 100 m centered at the edge. In the present numerical results, we compare three different wedge angles (α = 300°, 270°, 210°) for various incident angles. As seen in Figs. 3 to 5, the magnitude of the proposed solution is very similar to Luebbers' solution. After testing at different values of $\varphi_0(\gamma_0 = 0^0)$, we found that our proposed solution agrees well with the rigorous solution, except within a very limited region. A clear difference between the proposed and rigorous solutions can be seen in the illumination and shadow regions, near the shadow/reflection boundaries for different angles of incidence φ_0. Moreover, the proposed solution is closer to Maliuzhinets' solution than Luebbers' solution for a given wedge angle (Fig. 3).

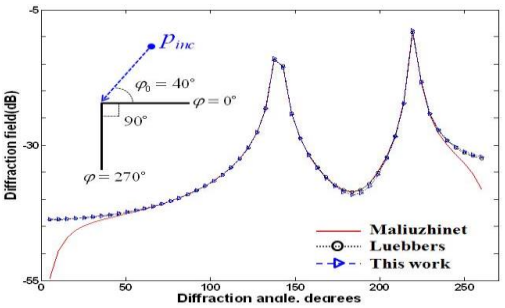

(a)

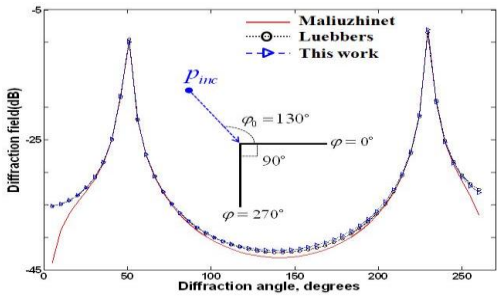

(b)

Fig. 4. Comparison of different diffraction fields for wedge angle α = 270°.
(a) Incident angle φ_0 =4 0° (one face) and (b) Incident angle φ_0 = 130° (two faces).

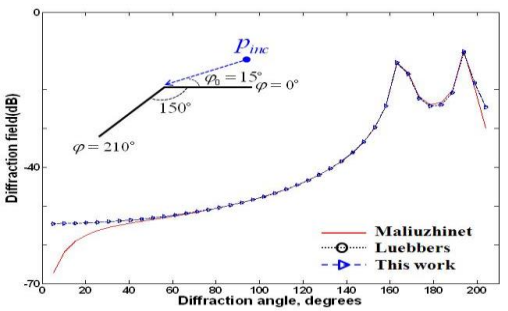

(a)

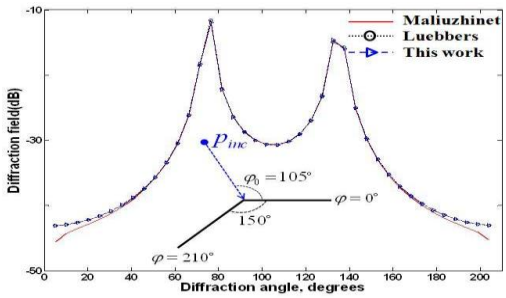

(b)

Fig. 5. Comparison of different diffraction fields for wedge angle α = 210°.
(a) Incident angle φ_0 = 15° (one face) and (b) Incident angle φ_0 =105° (two faces).

Next, to test the accuracy of the proposed heuristic 3D PTD for an arbitrary impedance polygon, we compare the numerical results for the total field (i.e., the sum of the scattering and diffraction fields) using the heuristic PTD and those from the rigorous solution obtained using the boundary element method. As an example, we investigate plane wave scattering from a box. The box [depicted in the inset of Fig. 6(a)] is a 10 × 3 × 1 in^3 rectangular box modeled using 5878 rectangular facets, and the parameters of the incident field are chosen to be f = 1 kHz, incident angle $\varphi_0 = 0^0, \gamma_0 = 0^0$ QUOTE $\gamma_0 = 0°, \varphi_0 = 0°$ **D**. The distance from the source to the origin of the employed coordinates is 1000 m [Fig. 6(a)]. The observation regions are on the xz-plane (γ = -70°~70°, ϑ = 0°) and yz-plane (γ = -70°~70°, ϑ = 90°). The points are located around an arc in steps of 1°, with a radius of 1000 m centered at the origin.

The impedance of the scatterer is the same as for the previous wedge (glass). As a reference for the rigorous solution we used SYSNOISE [25] software based on the boundary element method (BEM). The results obtained by this simulation were validated by comparing the scattering patterns extracted from the BEM code. Fig. 6 shows the scattering patterns in the xz- and yz-planes generated by the two methods and compared at f = 1 kHz. For the 3D impedance polygon, the results of this work agree well with the rigorous solution, except within a very limited region.

5. Conclusion

This paper described a newly proposed diffraction model for an arbitrary impedance polygon, which applies a heuristic modification to the physical theory of diffraction (PTD). Numerical results were presented that showed the usefulness and accuracy of the proposed method for the 2D wedge and 3D impedance polygon.

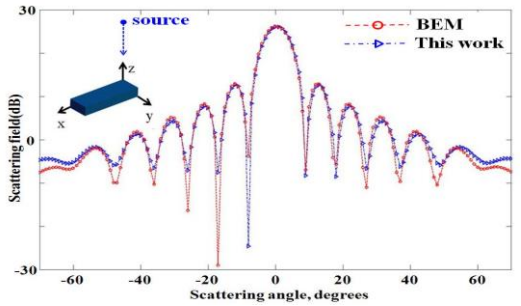

(a)

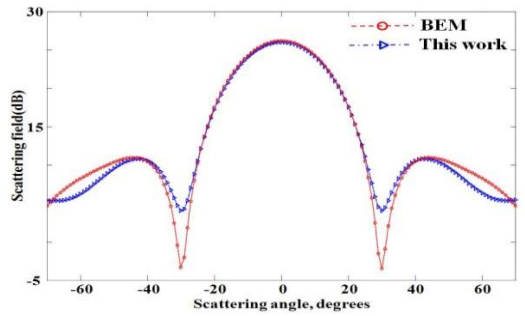

(b)

Fig. 6. Scattering patterns of 10 × 3 × 1 box modeled with 5878 rectangular facets
in (a) xz-plane at f = 1 kHz and (b) yz-plane at f = 1 kHz.

The proposed model was verified in relation to the accuracy of the solution and the application to a real impedance polygon by comparing its results with the numerical results from the rigorous Maliuzhinets' solution and BEM solution.

Appendix A. PTD coefficients of Ufimtsev for soft/hard wedge

In the coordinates of Fig. 1, the 3D PTD coefficients for a soft or hard wedge are given by [3]:

$$F_s^{(1)} = -[U(\sigma_1,\varphi_0) + U(\sigma_2,\alpha-\varphi_0)]\sin^2\gamma_0 \tag{A.1}$$

and

$$F_h^{(1)} = -[V(\sigma_1,\varphi_0)\sin\varphi + V(\sigma_2,\alpha-\varphi_0)\sin(\alpha-\varphi)]\sin\gamma_0\sin\vartheta \tag{A.2}$$

In the above relations, U and V are calculated using the following equations.

- $U(\sigma_1,\varphi_0) = U_t(\sigma_1,\varphi_0) - U_0(\sigma_1,\varphi_0)$. (A.3)
- $V(\sigma_1,\varphi_0) = V_t(\sigma_1,\varphi_0) - V_0(\sigma_1,\varphi_0)$. (A.4)
- $U_t(\sigma_1,\varphi_0) = \frac{\pi}{2\alpha\sin^2\gamma_0}\left[\cot\frac{\pi(\sigma_1+\varphi_0)}{2\alpha} - \cot\frac{\pi(\sigma_1-\varphi_0)}{2\alpha}\right]$ (A.5)
- $U_0(\sigma_1,\varphi_0) = \frac{\varepsilon(\varphi_0)}{2\sin^2\gamma_0}\left[\cot\frac{\sigma_1+\varphi_0}{2} - \cot\frac{\sigma_1-\varphi_0}{2}\right]$ (A.6)
- $V_t(\sigma_1,\varphi_0) = \frac{\pi}{2\alpha\sin^2\gamma_0\sin\sigma_1}\left[\cot\frac{\pi(\sigma_1+\varphi_0)}{2\alpha} + \cot\frac{\pi(\sigma_1-\varphi_0)}{2\alpha}\right]$ (A.7)
- $V_0(\sigma_1,\varphi_0) = \frac{\varepsilon(\varphi_0)}{2\sin^2\gamma_0\sin\sigma_1}\left[\cot\frac{\sigma_1+\varphi_0}{2} + \cot\frac{\sigma_1-\varphi_0}{2}\right]$ (A.8)
- Here, $\varepsilon(\varphi_0) = \begin{cases}1, & 0<\varphi_0<\pi\\ 0, & otherwise\end{cases}$, $\cos\beta_1 = \sin\gamma_0\sin\vartheta\cos\varphi - \cos\gamma_0\cos\vartheta$,
- and $\cos\sigma_1 = \frac{\cos^2\gamma_0 - \cos\beta_1}{\sin^2\gamma_0}$.

Appendix B. Heuristic UTD coefficients of Luebbers

The 2D heuristic diffraction coefficient from Luebbers is written as follows [6]:

$$\begin{aligned} D(\varphi,\varphi_0) = &-\frac{\pi}{2\alpha}\left[\cot\left(\frac{\pi+(\varphi-\varphi_0)}{2\alpha/\pi}\right)F(kLa^+(\varphi-\varphi_0))\right.\\ &+\cot\left(\frac{\pi-(\varphi-\varphi_0)}{2\alpha/\pi}\right)F(kLa^-(\varphi-\varphi_0))\\ &+\hat{R}_0(\varphi_0)\cot\left(\frac{\pi-(\varphi+\varphi_0)}{2\alpha/\pi}\right)F(kLa^-(\varphi+\varphi_0))\\ &\left.+\hat{R}_n(\alpha-\varphi)\cot\left(\frac{\pi+(\varphi+\varphi_0)}{2\alpha/\pi}\right)F(kLa^+(\varphi+\varphi_0))\right] \end{aligned}$$

(B.1)

where L is a distance parameter dependent on the nature of the incident wave,

$$F(x) = -2j\sqrt{x}e^{-jx}\int_{\sqrt{x}}^{\infty} e^{j\tau^2}d\tau \tag{B.2}$$

and

$$a^{\pm} = 2\cos^2\left(\frac{2\alpha N^{\pm} - \kappa}{2}\right) \tag{B.3}$$

In Eq. (B.3), $N^{\pm}$ are integers and most nearly satisfy

$$2\alpha N^{\pm} - \kappa = \pm\pi \tag{B.4}$$

Eq. (B.1) is slightly different from Eq. (5) from Luebbers' work, in that the notation is changed in accordance with the acoustic problem, and the directivity pattern of the original form is only considered for comparison with our heuristic PTD

References

[1] J. B. Keller, Geometrical theory of diffraction, J. Opt. Soc. Amer. 52 (1962) 116-130.
[2] R. G. Kouyoumjian, P. H. Pathak, A uniform geometrical theory of diffraction for an edge in a perfectly conducting surface, Proc. IEEE. 62 (1974) 1448-1461.
[3] P. Ya. Ufimtsev, Fundamentals of the Physical Theory of Diffraction , Wiley-IEEE, 2007.
[4] G. D. Maliuzhinets, Excitation, reflection and emission of surface waves from a wedge with given face impedances, Sov. Phys. Dokl. 3 (1958) 752-755.
[5] M. I. Herman, J. L. Volakis, T. B. A. Senior, Analytic expressions for a function occurring in diffraction theory, IEEE Trans. Antennas Propag. AP-35 (1987) 1083-1086.
[6] R. J. Luebbers, Finite conductivity uniform UTD versus knife diffraction prediction of propagation path loss, IEEE Trans. Antennas Propag. AP-32 (1984) 70-76.
[7] R. J. Luebbers, A heuristic UTD slope diffraction coefficient for rough lossy wedges, IEEE Trans. Antennas Propag. 37 (1989) 206-211.
[8] P. Holm, A new heuristic UTD diffraction coefficient for non-perfectly conducting wedges, IEEE Trans. Antennas Propag. 48 (2000) 1211-1219.
[9] H. M. El-Sallabi, I. T. Rekanos, P. Vainikainen, A new heuristic diffraction coefficient for dielectric wedges at normal incidence, IEEE Antennas Wireless Propag. Lett. 1 (2002) 165-168.
[10] H. M. El-Sallabi, P. Vainikainen, Improvement to diffraction coefficient for non-perfectly conducting wedges, IEEE Trans. Antennas Propag. 53 (2005) 3105-3109.
[11] D.a N. Schettino, F. Moreira, K. Borges, C. Rego, Novel Heuristic UTD Coefficients for the Characterization of Radio Channels, IEEE Trans. on Magnetics. 43 (2007) 1301-1304.
[12] S. K. Soni, A. Bhattacharya, New heuristic diffraction coefficient for modeling of wireless channel, Prog. in Electromag. Res. 12 (2010) 125-137.
[13] T. Lertwiriyaprapa, P. H. Pathak, J. L. Volakis, An approximate UTD ray solution for the radiation and scattering by antennas near a junction between two different thin planar material slab on ground plane, Prog. in Electromag. Res. 102 (2010) 227-248.
[14] Sanjay Soni, Amitabha Bhattacharya, Novel three-dimensional dyadic diffraction coefficient for wireless channel, Microwave and Opt. Tech. Lett. 52 (2010) 2132-2136.
[15] Daniela N. Schettino, Fernando J. S. Moreira, Cassio G. Rego, Heuristic UTD Coefficients for electromagnetic scattering by lossy conducting wedges, Microwave and Opt. Tech. Lett. 52 (2010) 2657-2662.
[16] Ayza Ghorbani, Ali Tajvidy, Emad Torabi, Reza Arablouei, A New Uniform Theory of Diffraction Based Model for Multiple Building Diffraction in the Presence of Trees, Electromagnetics. 31 (2011) 127-146.
[17] J. F. Legendre, T. Marsault, T. Vele, D. Cueff, Heuristic uniform 2D double wedge diffraction based on generalized Fresnel integral, Microwave and Opt. Tech. Lett. 53 (2011) 1841-1846.
[18] D. Klement, J. Preissner, V. Stein, Special problems in applying the physical optics method for backscatter computation of complicated objects, IEEE Trans. Antennas Propag. 36

(1988) 228-237.

[19] K. Kim, J. Cho, J. Kim, D. Cho, A fast estimation of sonar cross section of acoustically large and complex underwater targets using a deterministic scattering center model, Appl. Acoust. 70 (2009) 653-660.

[20] K. Kim, J. Kim, D. Cho, W. Seong, Applying time domain physical optics to acoustic wave backscattering problem, Appl. Acoust. 71 (2010) 321-327.

[21] P. Ya. Ufimtsev, Elementary edge waves and the physical theory of diffraction, Electromagnetics. 11 (1991) 127-160.

[22] A. Sommerfeld, Mathematische Theorie der Diffraction, Math. Ann. 47 (1896) 317-374.

[23] K. Lee, W. Seong, Y. Joo, Modeling of scattering from targets in an oceanic waveguide using Kirchhoff/diffraction method, J. Acoust. Soc. Am. 123 (2008) 3757.

[24] K. Lee, W. Seong, Time-domain Kirchhoff model for acoustic scattering from an impedance polygon facet, J. Acoust. Soc. Am. 126 (2009) EL14.

[25]SYSNOISE Rev 5.6, Users Manual, LMS International N.V.